Highly-stable monolithic femtosecond Yb-fiber laser system based on photonic crystal fibers

Liu, Xiaomin; Lægsgaard, Jesper; Turchinovich, Dmitry

Published in:
Optics Express

Link to article, DOI:
10.1364/OE.18.015475

Publication date:
2010

Document Version
Publisher's PDF, also known as Version of record

Highly-stable monolithic femtosecond Yb-fiber laser system based on photonic crystal fibers

Xiaomin Liu, Jesper Lægsgaard, and Dmitry Turchinovich*

DTU Fotonik - Department of Photonics Engineering,
Technical University of Denmark, DK-2800 Kgs. Lyngby, Denmark

**dmtu@fotonik.dtu.dk*

Abstract: A self-starting, passively stabilized, monolithic all-polarization-maintaining femtosecond Yb-fiber master oscillator / power amplifier with very high operational and environmental stability is demonstrated. The system is based on the use of two different photonic crystal fibers. One is used in the oscillator cavity for dispersion balancing and nonlinear optical limiting, and another one is used for low-nonlinearity final pulse recompression. The chirped-pulse amplification and recompression of the 232-fs, 45-pJ/pulse oscillator output yields a final direct fiber-end delivery of 7.3-nJ energy pulses of around 297 fs duration. Our laser shows exceptional stability. No Q-switched modelocking events were detected during 4-days long observation. An average fluctuation of only $7.85 \cdot 10^{-4}$ over the mean output power was determined as a result of more than 6-hours long measurement. The laser is stable towards mechanical disturbances, and maintains stable modelocking in the temperature range of at least 10 – 40 ^{0}C.

OCIS codes: (060.3510) Fiber lasers; (140.7090) Ultrafast lasers; (060.5295) Photonic crystal fibers; (140.3425) Laser stabilization; (320.5520) Pulse compression; (060.7140) Ultrafast processes in fibers.

References and links

1. K. Kieu, W. Renninger, A. Chong, and F. Wise, "Sub-100 fs pulses at watt-level powers from a dissipative-soliton fiber laser," Opt. Lett. **34**, 593–595 (2009).
2. D. Turchinovich, X. Liu, and J. Lægsgaard, "Monolithic all-PM femtosecond Yb-fiber laser stabilized with a narrow-band fiber Bragg grating and pulse-compressed in a hollow-core photonic crystal fiber," Opt. Express **16**, 14004–14014 (2008).
3. J. Lægsgaard, "Control of fiber laser mode-locking by narrow-band Bragg gratings," J. Phys. B **41**, 095401 (2008).
4. J. Limpert, T. Schreiber, S. Nolte, H. Zellmer, and A. Tünnermann, "All fiber chirped-pulse amplification system based on compression in air-guiding photonic bandgap fiber," Opt. Express **11**, 3332–3337 (2003).
5. M. E. Fermann, V. I. Kruglov, B. C. Thomsen, J. M. Dudley, and J. D. Harvey, "Self-similar propagation and amplification of parabolic pulses in optical fibers," Phys. Rev. Lett. **84**, 6010–6013 (2000).
6. H. Lim, F. Ilday, and F. Wise, "Femtosecond ytterbium fiber laser with photonic crystal fiber for dispersion control," Opt. Express **10**, 1497–1502 (2002)
7. C. K. Nielsen, K. G. Jespersen, and S. R. Keiding, "A 158 fs 5.3 nJ fiber-laser system at 1 m using photonic bandgap fibers for dispersion control and pulse compression," Opt. Express **14**, 6063–6068 (2006)
8. http://www.batop.de/products/saturable-absorber/saturable-absorber-mirror/data-sheet/saturable-absorber-mirror-1040nm/saturable-absorber-mirror-SAM-1040-40-500fs.pdf
9. http://www.nufern.com/fiber_detail.php/84

#125581 - $15.00 USD Received 16 Mar 2010; revised 5 May 2010; accepted 1 Jul 2010; published 7 Jul 2010

10. J. K. Lyngsø, B. J. Mangan, and P. J. Roberts,"Polarization maintaining hybrid TIR/bandgap all-solid photonic crystal fiber," in Conference on Lasers and Electro-Optics/Quantum Electronics and Laser Science Conference and Photonic Applications Systems Technologies, OSA Technical Digest (CD) (Optical Society of America, 2008), paper CThV1.
11. C. B. Olausson, C. I. Falk, J. K. Lyngsø, B. B. Jensen, K. T. Therkildsen, J. W. Thomsen, K. P. Hansen, A. Bjarklev, and J. Broeng, "Amplification and ASE suppression in a polarization-maintaining ytterbium-doped all-solid photonic bandgap fibre," Opt. Express **16**, 13657–13662 (2008).
12. J. Y. Lee and D. Y. Kim, "Versatile chromatic dispersion measurement of a single mode fiber using spectral white light interferometry," Opt. Express **14**, 11608–11615 (2006).
13. H. A. Haus, K. Tamura, L. E. Nelson and E. P. Ippen, "Stretched-pulse additive pulse mode-locking in fiber ring lasers: theory and experiment," IEEE J. Quantum Electron. **31**, 591–598 (1995).
14. S. Namiki, E. P. Ippen, H. A. Haus, and C. X. Yu, "Energy rate equations for mode-locked lasers," J. Opt. Soc. Am. B **14**, 2099–2111 (1997).
15. X. Liu, J. Lægsgaard, and D. Turchinovich, "Self-stabilization of a mode-locked femtosecond fiber laser using a photonic bandgap fiber," Opt. Lett. **35**, 913–915 (2010).
16. http://www.nufern.com/specsheets/pm980130014xx1550hp.pdf
17. http://www.crystal-fibre.com/datasheets/HC-1060-02.pdf
18. J. T. Kristensen, A. Houmann, X. Liu, and D. Turchinovich, "Low-loss polarization-maintaining fusion splicing of single-mode fibers and hollow-core photonic crystal fibers, relevant for monolithic fiber laser pulse compression," Opt. Express **16**, 9986–9995 (2008).
19. K. L. Sala, G. A. Kenney-Wallace, and G. E. Hall, "CW autocorrelation measurements of picosecond laser pulses," IEEE J. Quantum Electron. **QE-16**, 990–996 (1980).
20. J. Lægsgaard and P. J. Roberts, "Dispersive pulse compression in hollow-core photonic bandgap fibers," Opt. Express **16**, 9628–9644 (2008).
21. P. J. Roberts, private communication.
22. T. C. Newell, P. Peterson, A. Gavrielides, and M. P. Sharma, "Temperature effects on the optical properties of Yb-doped optical fibers," Opt. Commun. **273**, 256–259 (2007).
23. J. Mangeney, N. Stelmakh, F. Aniel, P. Boucaud, and J.-M. Lourtioz, "Temperature dependence of the absorption saturation relaxation time in light- and heavy-ion-irradiated bulk GaAs," Appl. Phys. Lett. **80**, 4711–4713 (2002).
24. E. Le Cren, S. Lobo, S. Feve, J.-C. Simon, "Polarization sensitivity characterization under normal incidence of a multiple quantum wells saturable absorber nonlinear mirror as a function of the temperature of the chip," Opt. Commun. **254**, 96–103 (2005).
25. H. Tu and S. A. Boppart, "Versatile photonic crystal fiber-enabled source for multi-modality biophotonic imaging beyond conventional multiphoton microscopy," Proc. SPIE **7569**, 75692CD-1–9 (2010).

1. Introduction

Femtosecond (fs) fiber lasers hold the promise of replacing current solid-state based fs lasers with sources being much cheaper, more robust, highly stable, and easy to operate by untrained staff. Such laser systems could find many applications in biomedical optics (e.g. as seeds for supercontinuum sources or pumps for many-photon experiments), precision micromachining, and basic research. Recent progress in the development of fs fiber lasers has resulted in pulse energies and durations comparable to the solid-state lasers. The environmental and operational stability of the laser is crucial for applications in medicine, micromachining, and metrology. However, the comments on stability of femtosecond fiber lasers are largely avoided in the literature. Many of the demonstrated lasers are laboratory-based, table-top systems, at least partly relying on the technology typical for the solid-state lasers, such as free-space coupling and mechanical adjustment.

In order to achieve high environmental and operational stability of the laser, free-space coupling of fibers and fiber elements should be avoided and self-stabilization mechanisms must be present to ensure stable modelocked operation. Also, direct fiber-end delivery of femtosecond pulses without the use of external pulse recompression in gratings or prisms is an important advantage.

Different cavity designs, modelocking (ML) and stabilization principles were demonstrated so far. ML schemes using nonlinear polarization rotation for pulse intensity management usually have a built-in power limiting mechanism, because the cavity loss is an oscillating function

#125581 - $15.00 USD Received 16 Mar 2010; revised 5 May 2010; accepted 1 Jul 2010; published 7 Jul 2010

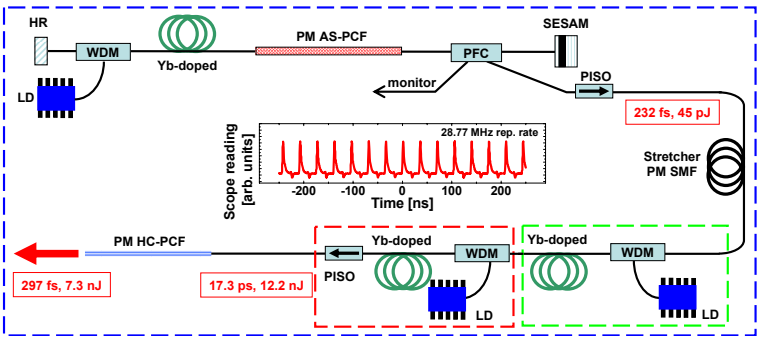

Fig. 1. General layout of the MOPA. HR - high-reflectivity broadband mirror, SESAM - semiconductor saturable absorber mirror, PM AS-PCF - PM all-solid photonic crystal fiber, WDM - 980/1030 nm wavelength division multiplexer, PFC - 20/80 polarization filter coupler, LD - pump laser diode at 974 nm, PISO - polarization-maintaining isolator, PM SM - polarization-maintaining single-mode fiber. PM HC-PCF - PM hollow-core photonic crystal fiber. Inset: oscilloscope reading of the oscillator pulse train in fundamental single-pulse modelocking regime.

of pulse energy. Such lasers can provide multi-nJ output at sub-100 fs pulse durations [1]. However, the polarization rotation schemes typically involve some free-space components in the form of waveplates and polarizers. Also, this modelocking scheme usually relies on non-polarization maintaining fibers, which makes the modelocking stability susceptible to ambient temperature variation. On the other hand, lasers based on semiconductor saturable absorbers (SESAMs) can easily be made fully monolithic, and also have excellent self-starting properties, but in this case stabilization against detrimental Q-switching behavior requires a separate optical limiting mechanism. Our recent work demonstrated that fiber Bragg gratings can be used as an efficient stabilizing element, but at the price of reducing the pulse bandwidth to the sub-nm level, which results in a few picoseconds – long bandwidth-limited pulses [2, 3]. A monolithic oscillator with a higher bandwidth and transform-limited output would be highly desirable because it would allow the use of either chirped-pulse [4] or parabolic [5] amplification to generate high-power ps pulses suitable for dispersive recompression.

In this paper we demonstrate a highly stable femtosecond master oscillator / power amplifier (MOPA) operating around the wavelength of 1033 nm, based on the use of different types of photonic crystal fibers (PCFs). One is used intra-cavity for both oscillator dispersion management *and* stabilization. This stabilization is achieved by distributed nonlinear filtering and optical limiting, which results in exceptional environmental and operational stability of the system. One more PCF is used for a final low-nonlinearity compression of amplified laser pulses. Our system employs chirped pulse amplification (CPA) principle, where the output of the femtosecond oscillator is strongly stretched before amplification in order to preserve smoothness of the spectrum.

In [6] a PCF was used in a non-monolithic and non-PM cavity for dispersion compensation. A similar arrangement to ours, but based on non-PM fibers and partly using free-space coupling, was presented in [7]. However, the stability of this laser was comparable to ”that of other non-PM fiber lasers - that is the laser was not environmentally stable, and the output could be affected by moving the fibers”.

Our laser delivers the pulses with fixed polarization state, of 297 fs duration in the main peak, and 7.2 nJ total energy (of which 56 % is in the main peak). This performance is comparable to

#125581 - $15.00 USD Received 16 Mar 2010; revised 5 May 2010; accepted 1 Jul 2010; published 7 Jul 2010

some other published lasers. However, the operational and environmental stability of our laser is extremely high, which is crucial for most fiber laser applications. To the best of our knowledge, this is the first demonstration of a monolithic, non-table-top modelocked femtosecond system which maintains stable operation in the temperature range of at least 10-40 ^{0}C. This shows a potential of PCF-based technology in producing a highly stable modelocked femtosecond fiber lasers, as an alternative to other approaches such as e.g. use of fiber Bragg gratings.

2. Design and performance of the laser

Our fully monolithic laser consists of four main stages: a modelocked oscillator, a stretcher fiber, an amplifier stage featuring a pre-amplifier and a booster amplifier, and a spliced-on hollow-core photonic crystal fiber pulse compressor. All stages, including the compressor, were based on PM fibers, and were spliced together. The schematic of the laser is shown in Fig. 1.

The linear-cavity oscillator was confined between a fiber-pigtailed semiconductor saturable absorber mirror (SESAM) and a fiber-pigtailed broadband high-reflectivity mirror. The SESAM had a modulation depth 24 %, non-saturable loss of 16 %, saturation fluence of 130 μJ/cm^2, and relaxation time of 500 fs [8]. A 32-cm long Yb-doped fiber [9] was used as gain medium.

The cavity dispersion management was performed using 1.21 m of specialty PM all-solid photonic crystal fiber (PM AS-PCF) from Crystal Fibre A/S, which features anomalous dispersion at Yb wavelength. This fiber consists of fused SiO_2 core and matrix, and B:SiO_2 and Ge:SiO_2 rods, and is guiding using a hybrid mechanism: by total internal reflection (TIR) between SiO_2 core and B:SiO_2 rods in one plane, and by photonic bandgap mechanism provided by Ge:SiO_2 rods in the orthogonal plane [10, 11]. A scanning electron microscope (SEM) image of this fiber is shown in Fig. 2(a), and its transmission and dispersion spectra are shown in Fig. 2(b). The dispersion spectrum was estimated by spectral white light interferometry [12].

This fiber was instrumental in passive stabilization of our laser by introducing the nonlinear optical limiting mechanism for the stronger pulses that result from spontaneous and induced intensity fluctuations. This self-stabilization mechanism is based on the wavelength-dependent cavity loss for the laser, introduced by the AS-PCF. As the intracavity power grows, the stronger laser pulses experience stronger self-phase modulation (SPM) in the fibers, and their spectral bandwidth expands. In order to maintain the shorter pulse duration in a weakly-stretched pulse regime [13,14] such stronger and spectrally broader pulses are formed on the longer-wavelength side of the AS-PCF transmission spectrum, featuring higher anomalous dispersion. On the other hand, the transmission loss of the AS-PCF is also higher in this spectral range, which leads to efficient optical limiting for such pulses, and to the delayed onset of Q-switched modelocked operation. The detailed investigation of such a self-stabilization mechanism of a modelocked femtosecond fiber laser with a photonic crystal fiber is presented in [15].

The rest of the cavity consisted of a standard PM single mode fiber (SMF) [16], and the total cavity length was 3.55 m, which resulted in the fundamental repetition rate of 28.77 MHz (see inset of Fig. 1). The cavity was pumped by a 974 nm single-mode laser diode through a 980/1030 wavelength division multiplexer (WDM), and for the outcoupling a 20/80 2x2 polarization filter coupler (PFC) was used. The oscillator had two outputs: one was isolated, stretched, and used for seeding the amplifier, and another one was angle-cleaved and used as a monitor port for stability observations.

The laser operated in a weakly-stretched pulse regime [13, 14] with small anomalous cavity dispersion. The net cavity dispersion on one roundtrip was estimated to be zero at 1024 nm, and at the laser central operating wavelength of 1033 nm it was 0.089 ps/nm [15]. The laser was self-starting, and provided stably modelocked pulses with the energies in the range 39-49 pJ, in the pump power range of 65-75 mW. At higher pump powers the laser enters a Q-switched ML phase, followed by a stable harmonic ML phase. The oscillator-generated pulses measured after

#125581 - $15.00 USD Received 16 Mar 2010; revised 5 May 2010; accepted 1 Jul 2010; published 7 Jul 2010

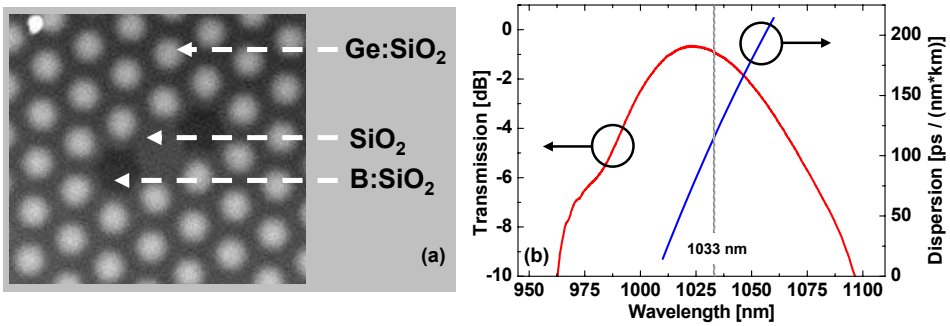

Fig. 2. (a) SEM image of the PM AS-PCF. Courtesy of Crystal Fibre A/S. (b) Transmission and dispersion of PM AS-PCF. Central wavelength of the laser at 1033 nm is indicated by a grey line.

1-m long PM SMF pigtail following the outcoupler, had near-perfect Gaussian shapes with no side pulse visible in the autocorrelation, and at 45 pJ energy the pulse duration was estimated to be 232 fs at full width at half maximum (FWHM) from the autocorrelation with FWHM of 328 fs [15].

We note here, that at the outcoupling point the pulses were still negatively chirped, and were recompressed down to 232 fs during the propagation in the 1-m long PM SMF pigtail. We will discuss this recompression, as well as spectral and temporal evolution of the intra-cavity pulses in the oscillator cavity in the Theoretical section below.

The isolated output of the master oscillator was launched into a 35-m long standard PM SMF, where the laser pulse was stretched to approximately 12 ps duration, in order to decrease its peak intensity before amplification. The stretched pulse was amplified in a chain of two single-mode amplifiers to the energy of 12.7 nJ, corresponding to a cw equivalent power of 365 mW. After the isolation, the pulse energy was 12.2 nJ (351 mW of cw power). The pulse shape had the autocorrelation of 24.5 ps at FWHM, corresponding to 17.3 ps in pulse duration at FWHM, assuming Gaussian shape. The spectral bandwidth of the oscillator input pulse was 7 nm at FWHM, and after CPA and isolation it was 9 nm.

After isolation, the stretched and amplified laser signal was launched into a compressor - a hollow-core photonic crystal fiber (HC-PCF) HC-1060-2 from Crystal Fibre A/S [17], featuring anomalous dispersion at the laser wavelength. Such a fiber has a group birefringence of $\Delta n = 1.65 \cdot 10^{-4}$, which ensures its high PM properties [18]. This HC-PCF was fusion-spliced onto the PM SMF output of the amplifier isolator with the splice loss of 0.6 dB using the technique described in [18].

After propagation through 21 m of HC-PCF, we achieved the shortest pulse duration with an autocorrelation of 420 fs at FWHM, and an estimated pulse duration of 297 fs. The spectral bandwidth of the compressed output pulse was found to be 10 nm at FWHM. The resulting cw output power was 210 mW, corresponding to a pulse energy of 7.3 nJ. The total compressor loss, including PM-SMF-to-HC-PCF splice loss was 2.2 dB, of which 1.6 dB was attenuation in HC-PCF. The HC-PCF attenuation coefficient was 0.076 dB/m.

We now show the evolution of the laser pulse throughout the system in the temporal and spectral domains, respectively. In the time domain, shown in Fig. 3(a), an oscillator-generated near-perfect Gaussian pulse with FWHM duration of 232 fs acquires the duration of 17.3 ps after CPA, and is finally recompressed to the duration of 297 fs. The conversion factors from work [19] were used to estimate the pulse durations from the measured autocorrelations.

#125581 - $15.00 USD Received 16 Mar 2010; revised 5 May 2010; accepted 1 Jul 2010; published 7 Jul 2010

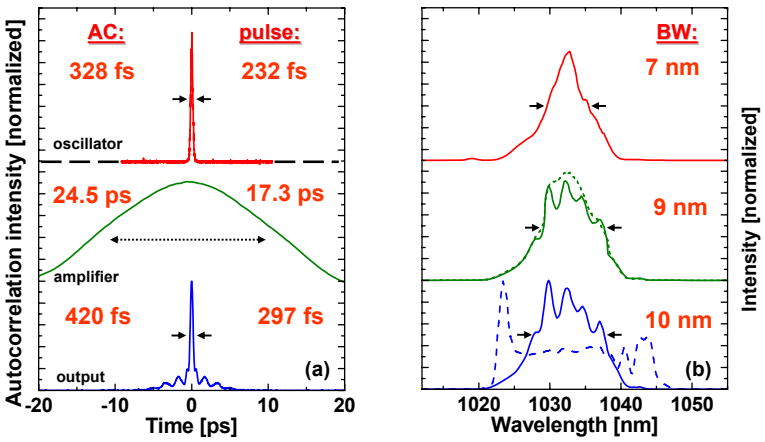

Fig. 3. (a) Autocorrelations of the pulse measured after 1-m long PM SMF pigtail following the output port of the oscillator (45 pJ / 1.35 mW), at the isolated output of the amplifier before compression in HC-PCF (12.2 nJ / 351 mW), and at the output of the MOPA after compression in HC-PCF (7.3 nJ / 210 mW). Corresponding autocorrelation and pulse durations at FWHM are indicated. (b) Corresponding optical spectra. Spectral bandwidth at FWHM is indicated. Dotted line - amplifier spectrum measured before the isolator. Dashed line - output spectrum in the case when no CPA is used, i.e. the oscillator pulses are not stretched before amplification. See text for details.

The final pulse, however, is accompanied by little side pulses, as a result of residual chirp by non-compensated third-order dispersion in the HC-PCF, as well as by the spectral oscillations present in the isolated amplifier output. The pulse quality can be further significantly improved by achieving the parabolic amplification. In the work [5] it is shown theoretically and experimentally that near-parabolic pulses can be obtained by amplifying 200-fs input pulses in normal-dispersion fibers. Our recent work [20] shows that parabolic pulses may be compressed with high quality ($>$ 90 % of the pulse energy in the main peak) at pulse energies of tens of nJ, when using a suitable (but realistic) hollow-core compressor fiber. This suggests that our approach can be further improved substantially before being limited by dispersion-slope effects.

In the spectral domain, shown in Fig. 3(b), the oscillator delivers a smooth spectrum with the bandwidth of 7 nm at FWHM, which then undergoes spectral broadening to 9 nm after CPA due to SPM in the amplifier fibers. The amplifier spectrum before isolation, shown by the dotted line, is smooth. However, after the isolator, the spectrum develops spikes, possibly due to spectral filtering in the isolator itself. The spectrum of the pulse compressed in 21 m of HC-PCF is very similar to that of the isolated amplifier output. However, its spectral bandwidth is now slightly larger and reaches 10 nm at FWHM. This low Kerr nonlinearity of the HC-PCF is in accordance with our earlier observations [2]. However, we note here that at the pulse energies reaching several nJ, and the pulse durations of only few hundred fs, as in this work, the Kerr nonlinearity of HC-PCF already becomes observable. The importance of using CPA for maintaining a relative spectral smoothness is shown by the example of an output spectrum in the case, where the seed pulse was launched into the amplifier without stretching [dashed line in Fig. 3(b)]. This spectrum is very strongly distorted by the SPM.

#125581 - $15.00 USD Received 16 Mar 2010; revised 5 May 2010; accepted 1 Jul 2010; published 7 Jul 2010

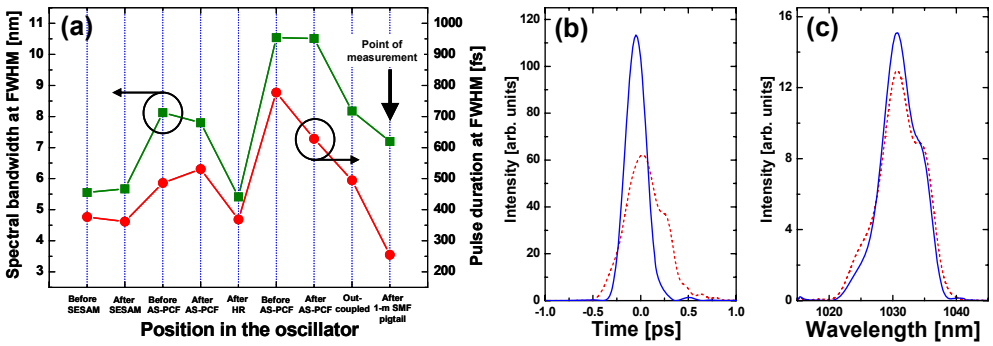

Fig. 4. (a) Calculated evolution of spectral bandwidth and pulse duration in the oscillator on one roundtrip, and after 1-m long PM SMF pigtail following the outcoupler (point of experimental measurements). (b) Calculated pulse shapes at the outcoupler (dashed line), and at the point of measurements (solid line). (c) Corresponding spectra.

3. Master oscillator theoretical modelling

A detailed model of the master oscillator was set up along the lines described in [3]. The SESAM was described by a rate equation model using the parameters given above, the amplifier was approximated by a point amplifier surrounded by passive fibers with the proper dispersion values, and propagation in passive fibers was described by a generalized nonlinear Schrödinger equation. The inclusion of third-order dispersion is particularly important due to the careful dispersion balancing in the cavity, and the strong third-order dispersion of the AS-PCF. The dispersion parameters for the standard PM fibers were taken to be β_2=0.023 ps^2/m, β_3=3.9·10^{-5} ps^3/m [7], and the effective area was assumed to be 28 μm^2, corresponding to an MFD of 6 μm. For the amplifier fiber, the dispersion values were taken as β_2=0.039 ps^2/m and β_3=10^{-5} ps^3/m [9]. The dispersion parameters of the AS-PCF were measured to be β_2=-0.0577 ps^2/m, β_3=0.00133 ps^3/m, and its effective area was estimated to be 88 μm^2 from numerical modelling [21]. The high β_2 and β_3 values of the AS-PCF reflect a complex and rapidly changing mode profile, which also imposes a splice loss to the standard PM fibers, with a significant frequency dependence. The measured insertion loss curve was included in the modelling and found to be crucial for explaining the excellent stability properties of the laser [15].

The model results reproduce most features of the experimental spectra, although the pulse energy where stable ML operation occurs is somewhat underestimated (around 30 pJ in the model). We attribute this discrepancy to differences in fiber effective area parameters, and possibly also SESAM parameters, between model and experiment. The modelling reveals a significant intracavity pulse breathing, with both temporal and spectral FWHM varying by about a factor of two, as shown in Fig. 4(a). Since the pulse seeks to optimize SESAM transmission, it is approximately transform limited at the SESAM, and by consequence also at the HR mirror at the opposite end of the cavity. This implies that the pulse has negative chirp at the outcoupling point, and will therefore recompress in a standard fiber with normal dispersion, such as the isolator pigtails used in the experiment. Interestingly, the calculated pulse duration after 1 m of pigtail is significantly shorter than the pulse width at any point in the cavity. This can be explained by the spectral recompression effect, occuring when a negatively chirped pulse propagates in a medium with a positive Kerr coefficient. From Fig. 4(a) it can be seen that the bandwidth of the cavity pulse decreases from 8.2 nm to 5.5 nm upon propagation from the point of output coupling to the SESAM. The outcoupled pulse, on the other hand, is four times

#125581 - $15.00 USD Received 16 Mar 2010; revised 5 May 2010; accepted 1 Jul 2010; published 7 Jul 2010

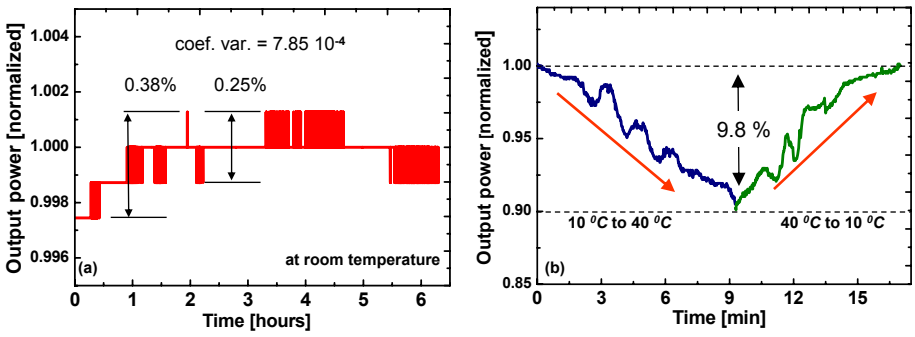

Fig. 5. Output power of the oscillator in stable fundamental modelocking regime as (a) a function of lab time, measured at room temperature; (b) during reversible temperature sweeps in the range 10-40 ^{0}C. Here temperature was not changing evenly with time.

weaker and therefore only recompresses to about 7.2 nm. It is noted that the calculated pulse after 1-m long pigtail is almost transform limited, and that both the calculated pulse duration (255 fs) and bandwidth (7.2 nm) are in very good agreement with the measured values (232 fs and 7 nm, respectively). In Fig. 4(b,c) the pulse shapes and spectra right at the outcoupler and after 1 m pigtail propagation are shown. Note that the pulse shape in both the temporal and spectral domains has significant deviations from an ideal gaussian or *sech*^{2} shape, suggesting that simplified models of stretched-pulse cavities based on such assumptions might not be applicable in this case.

4. Stability measurements

We have performed stability test of the oscillator by monitoring the output power during at least 6 hours of operation in the stably modelocked regime at room temperature, see Fig. 5(a). We have observed a slight rise of the output power during the first hour of operation, which can be attributed to a thermal readjustment of the pump diode. This initial output power rise amounts to a maximum output power fluctuation of only 0.38 %. In the following 5 hours of observations we noticed even smaller maximum output power fluctuations amounting to only 0.25 %. The ”quantization” of the output measurement is caused by the discrete data acquisition scheme, available to us in this experiment. Based on these measurements we calculated the coefficient of variation over mean output power in the whole observation period. It was found to be only $7.85 \cdot 10^{-4}$, which is the long-term stability of our laser. This is a good result for a passively-stabilized monolithic, non-table-top femtosecond fiber laser system.

The overall modelocking stability of our laser was tested during 4-days long continuous operation, revealing no Q-switched modelocking events during this period. The laser remains stable against mechanical disturbances such as moving and reshuffling the fibers and kicking the tray on which the system rests. The laser operation can be disrupted by bending the fibers to around 1 cm of bending diameter, which results in higher cavity loss and puts the laser below threshold. Once such a strongly bent fiber is released, the laser fully resumes its stable operation.

We have also performed variable-temperature measurements by placing the laser in a temperature chamber and performing temperature sweeps in the maximally-possible range between 10 ^{0}C and 40 ^{0}C. The results of the temperature stability measurements are shown in Fig. 5(b). The laser was always operating in the stable modelocked regime in the whole temperature sweep range, which suggests that the actual thermal stability range is even larger. At an

#125581 - $15.00 USD Received 16 Mar 2010; revised 5 May 2010; accepted 1 Jul 2010; published 7 Jul 2010

increase of the temperature we observed an overall decrease in the output power, with a maximum power drop of 9.8 % at 40 ^{0}C. When the laser was cooled down back from 40 ^{0}C to 10 ^{0}C, the output power increased and reached the initial values, thus showing no hysteresis behavior. The output power decrease and increase during temperature sweeps was accompanied by the clearly visible oscillations, that we attribute to a known effect of the temperature-dependent polarization evolution in PM fiber splices. We note here, that the temperature was not changing evenly with time during these measurements, and only the starting and ending temperatures were known precisely. Thus, in Fig. 5(b) we are only able to plot the output power as a function of laboratory time.

The temperature dependence of Yb-ions emission and absorption cross-section [22], as well as the complex temperature-dependent effects in saturable absorber, affecting its recovery time and modulation depth [23, 24] all lead to the decrease of the laser output power at elevated temperatures. However, the stability of mode-locking, i.e. the absence of Q-switching events during long-term and temperature tests, is attributed to the presence of self-stabilization mechanism of the laser, relying on nonlinear optical limiting in the intra-cavity AS-PCF.

5. Conclusions

In conclusion, we demonstrated a monolithic femtosecond Yb-fiber MOPA using an all-solid PM PCF for dispersion management and stabilization of the master oscillator, and a PM HC-PCF for final pulse recompression. The self-starting, HC-PCF-compressed MOPA delivers 7.3-nJ pulses with the main peak of around 297 fs FWHM duration directly from the output fiber end. A signature of non-compensated third-order dispersion is present in the pulse. Our future attempts will be aimed at achieving a parabolic pulse compression in this laser system, that can result in an improved resulting pulse quality.

We have demonstrated a very high operational and environmental stability of the laser, resulting in less than 0.38 % output power fluctuations during more than 6 hours of operation, and maintained stable modelocking during temperature sweeps in the range 10 ^{0}C and 40 ^{0}C. The long-term stability of our laser, the coefficient of variation of output power, is only $7.85 \cdot 10^{-4}$ over more than 6 hours of measurements. The 4-days long observation of a stably modelocked laser revealed no Q-switched modelocking events during this period. We demonstrated that PCF technology can be a viable alternative to other methods such as e.g. FBGs in providing a monolithic and highly stable femtosecond fiber laser.

Such a laser has a potential in industrial and medical applications, where both high stability and direct fiber-end delivery of femtosecond pulses are required. High environmental stability could pave the way for use of this kind of a laser in a multi-modality biophotonics platform, such as suggested in [25].

We have performed theoretical modelling of the laser signal evolution within the master oscillator, which shows spectral and temporal breathing of the laser pulse during a cavity roundtrip. The experimentally observed oscillator pulse duration and its spectral bandwidth are in good agreement with the results of our theoretical modelling.

Acknowledgments

We would like to acknowledge Danish Advanced Technology Foundation (HTF) for financial support; L. Leick, T.V. Andersen, and D. Noordegraaf for valuable discussions and assistance in stability measurements; P. J. Roberts for supplying us with modeling data for the AS-PCF; and Crystal Fibre A/S (part of NKT Photonics) for providing the photonic crystal fibers.

#125581 - $15.00 USD Received 16 Mar 2010; revised 5 May 2010; accepted 1 Jul 2010; published 7 Jul 2010